

# Native Complex Formation between Apolipoprotein E Isoforms and the Alzheimer's Disease Peptide A $\beta$

Winnie Chan,<sup>‡</sup> James Fornwald,<sup>§</sup> Mary Brawner,<sup>§</sup> and Ronald Wetzel<sup>\*‡</sup>

Departments of Macromolecular Sciences and Gene Expression Sciences, SmithKline Beecham Pharmaceuticals, 709 Swedeland Road, King of Prussia, Pennsylvania 19406

Received December 4, 1995; Revised Manuscript Received March 5, 1996<sup>®</sup>

**ABSTRACT:** To explore whether the genetic linkage between apolipoprotein E (ApoE) alleles and susceptibility to Alzheimer's disease might be attributable to a direct molecular interaction between ApoE and the amyloid peptide A $\beta$ , we have produced ApoE variants in *Escherichia coli* and studied their interactions with A $\beta$  under native conditions. When incubated with A $\beta$  at 20–40  $\mu$ M concentrations, all three isoforms of ApoE (2, 3, and 4) readily form complexes with A $\beta$  which can be isolated by gel filtration in native buffer. Freshly mixed ApoE and A $\beta$  generate a complex that co-migrates in gel filtration with the main A<sub>280</sub> peak, which migrates identically to the ApoE tetramer alone. After several hours incubation, an additional, high molecular weight, soluble aggregate appears which also contains both ApoE and A $\beta$ . Neither ApoE nor A $\beta$  incubated by themselves produces high molecular weight aggregates under these conditions. Incubation of A $\beta$  with control proteins bovine serum albumin and immunoglobulin generates negligible binding in the gel filtration assay. Similar results were obtained whether A $\beta$ (1–40) or A $\beta$ (1–42) was used, and plasma-derived ApoE gave similar results to *E. coli*-produced material. The data are consistent with a role for ApoE–A $\beta$  interactions in modulating the development of AD. Since no major differences were observed in the behavior of the three ApoE isotypes, however, the molecular basis of the genetic trend between ApoE alleles and AD cannot be attributed to specific activity differences between the molecular forms of ApoE characterized in this study.

Apolipoprotein E is a homotetrameric, highly  $\alpha$ -helical protein primarily known for its involvement in cholesterol metabolism, in which it binds to lipoprotein particles and mediates, *via* a receptor binding surface on the ApoE,<sup>1</sup> cellular uptake of the complex, and its load of cholesterol (Weisgraber, 1994). The protein became implicated in Alzheimer's disease when it was detected immunochemically as a minor constituent of amyloid plaque (Namba et al., 1991; Wisniewski & Frangione, 1992). Recently, genetic studies (Corder et al., 1993) have implicated the ApoE gene as one of at least four (Selkoe, 1995) *loci* associated with familial Alzheimer's. There are three alleles of ApoE in the human population. ApoE3 is the major allele and is considered the wild type. Both minor alleles, 2 and 4, are associated with abnormalities in cholesterol metabolism (Weisgraber, 1994). It is now believed that ApoE4 is also associated with increased risk of developing Alzheimer's (Corder et al., 1993).

The genetics are supported by *in vitro* studies indicating ApoE binding to the amyloid peptide A $\beta$  (Strittmatter et al., 1993a,b; Wisniewski et al., 1993; LaDu et al., 1994, 1995) or to its fibrils (Sanan et al., 1994), as well as modulation

of A $\beta$  fibril formation by the addition of ApoE (Ma et al., 1994; Wisniewski et al., 1994; Castano et al., 1995; Evans et al., 1995). Although these studies are in general agreement that there is a physical interaction between ApoE and A $\beta$ , there is as yet no consensus on the nature of the interaction. One particular deficit in our knowledge is the absence of any data on complex formation in which the complex is both generated and quantified under native conditions in the solution phase. One reason for this lack of data is probably the poor behavior of A $\beta$  in solution. This peptide is not only prone to formation of amyloid fibrils (Kirschner et al., 1987) and other organized and amorphous aggregates (Hilbich et al., 1991; Sanan et al., 1994; Wood et al., 1996), it also has a tendency to adsorb to surfaces (W. Chan and R. Wetzel, unpublished observations) and associate nonspecifically with other proteins (Strittmatter et al., 1993a) due to its hydrophobic nature. These properties complicate quantitative transfer and measurement of the peptide.

In this paper we report an experimental approach to quantitation of native complex formation between ApoE alleles and A $\beta$  which relies on chromatographic isolation of complex by gel filtration, and quantitation of complex constituents by immunochemical dot blots. This procedure provides convincing evidence for two types of native complex, one involving binding of monomeric A $\beta$  and another involving binding of an aggregated form of A $\beta$ . We also show that the three allelic variants of ApoE all display about equivalent abilities to form these complexes. Since the results reveal strong interactions between A $\beta$  and ApoE, they are consistent with models of Alzheimer's disease etiology involving ApoE–A $\beta$  interactions. At the same time, these studies fail to identify in the ApoE–A $\beta$  interaction

\* To whom correspondence should be addressed at 1732 Hamilton Dr., Phoenixville, PA 19406.

<sup>‡</sup> Department of Macromolecular Sciences.

<sup>§</sup> Department of Gene Expression Sciences.

<sup>®</sup> Abstract published in *Advance ACS Abstracts*, May 1, 1996.

<sup>1</sup> Abbreviations: ApoE, apolipoprotein E; HFIP, 1,1,1,3,3,3-hexafluoro-2-propanol; PMSF, phenylmethylsulfonyl fluoride; IPTG, isopropyl  $\beta$ -D-thiogalactoside; EDTA, disodium ethylenediaminetetraacetic acid; Tris, tris(hydroxymethyl)aminomethane; LB, Luria broth; HOAc, acetic acid; PBS, phosphate-buffered saline; IgG, immunoglobulin; SDS, sodium dodecyl sulfate; PAGE, polyacrylamide gel electrophoresis; DTT, dithiothreitol; HRP, horseradish peroxidase.

any significant biochemical basis for the genetic trend between ApoE alleles and Alzheimer's disease. This implies that the allele-based discrimination must come into play at some other point in the physiological chemistry of this system.

## MATERIALS AND METHODS

**Materials.** The anti-A $\beta$  antibody 1E8 was a gift of Steve Holmes (SmithKline). The goat anti-human ApoE antibody was obtained from CalBiochem, and the peroxidase linked anti-immunoglobulin antibodies were obtained from Bio-Rad (goat anti-mouse) and Southern Biotechnology (rabbit anti-goat). The ApoE cDNA was obtained from Nabil Elshourbagy (SmithKline). Phosphate-buffered saline (PBS) was prepared from sodium and potassium phosphates and chlorides and adjusted to pH 7.4 according to the protocol in Sambrook et al. (1989). This PBS has sufficient buffering capacity to hold a pH of 7 or above after a 1:10 dilution of 0.1% HOAc.

**Construction and Expression of the ApoE Isoforms.** The human cDNA coding for the ApoE3 protein was subcloned into pALTER1, and site-directed mutagenesis was performed following the Altered Sites system (Promega). Oligonucleotides with the appropriate base changes were synthesized to introduce the single amino acid changes C112R or R158C into ApoE3 to generate ApoE isoforms 4 and 2, respectively. In a second round of mutagenesis, a stop codon was introduced after amino acid 191 for expression of the N-terminal portion of each protein. The ApoE DNAs were cloned in frame with the pectate lyase B (*pelB*) signal sequence in an *Escherichia coli* expression vector under the *tac* promoter. Plasmids pTPApoE2, pTpApoE3, and pTpApoE4, which harbor DNAs coding for the ApoE2, ApoE3, and ApoE4 proteins, respectively, were transformed into *E. coli* strain MM294 for expression. An overnight culture, inoculated from a single colony into LB media containing 100  $\mu$ g of ampicillin/mL and grown overnight at 37 °C, was diluted 1:40 into fresh media. The growth temperature was then lowered to 32 °C and when the culture density reached  $A_{600} = 1$ , IPTG was added to 1 mM final concentration. Cells were harvested after 3–4 hours of induction by centrifugation, and the cell pellets were stored at –80 °C.

**ApoE Purification.** The ApoE secreted into the periplasm was released by osmotic shock. The cell pellet from 4 L of culture  $A_{600} = \sim 2$  was resuspended in 400 mL of 20% sucrose, 30 mM Tris-HCl, 1 mM EDTA, pH 8.0, containing protease inhibitors at final concentrations of 1 mM PMSF, 1  $\mu$ M pepstatin A, and 10  $\mu$ M leupeptin. The cell suspension was incubated on ice for 20 min with occasional vortexing and then centrifuged at 10 K in a Sorvall GSA rotor for 20 min. The supernatant of the sucrose extraction was removed and saved to check for ApoE. The cell pellet was further extracted with 400 mL of ice-cold H<sub>2</sub>O supplemented with 1 mM EDTA and the protease inhibitors and centrifuged. To the supernatant of the water extraction, where the majority of the ApoE is found, 1 M Tris-HCl, pH 7.5, was added to 30 mM final concentration.

The ApoE in the water fraction was batch absorbed to Q-Sepharose (Sigma) for 2 h at 4 °C (10 mL of centrifuged resin/cell pellet from 1 L of cells,  $A_{600} = \sim 2$ ). The resin was then washed twice with 30 mM Tris-HCl, 1 mM EDTA, pH 7.5, before eluting the ApoE with 100 mL of 50 mM

NaH<sub>2</sub>PO<sub>4</sub>, 1 mM EDTA, 0.5 M NaCl, pH 7.5. The protein was then dialyzed into 25 mM NH<sub>4</sub>HCO<sub>3</sub>, 1 mM EDTA with protease inhibitors PMSF and pepstatin A at 4 °C overnight. The ApoE from the Q-Sepharose was further purified by passing it through a heparin-agarose type II affinity column (Sigma) previously equilibrated with 25 mM NH<sub>4</sub>HCO<sub>3</sub>, 1 mM EDTA. The column was washed with the equilibration buffer followed by 0.3 M NH<sub>4</sub>HCO<sub>3</sub>, 1 mM EDTA to remove other proteins, and the ApoE was eluted from the heparin column with 0.7 M NH<sub>4</sub>HCO<sub>3</sub>, 1 mM EDTA at ~90% purity (with respect to other Coomassie Blue staining proteins by SDS–PAGE).

The N-terminal domain of ApoE3 was purified according to the same procedure as the full-length molecule with minor modifications. In the osmotic shock procedure, the protein distributes into both the sucrose and the water fractions. These fractions were processed separately up to the heparin chromatography step, at which point they were combined. The N-terminal domain elutes from the heparin column at 0.3 M ammonium bicarbonate, giving a purity after this step of about 90% (SDS–PAGE, Coomassie Blue staining).

**Isolation of the A $\beta$ –ApoE Complex by Gel Filtration.** A $\beta$  was handled as follows. In general, vials of 5 mg of dry A $\beta$ (1–40) (Bachem) were dissolved in 0.1% HOAc at 1–2 mg/mL and aliquoted into microfuge tubes at 100  $\mu$ g per tube. These were spin-dried, and the dry peptide was stored at –80 °C until needed. With experiments requiring disaggregated peptide, A $\beta$ (1–40) and A $\beta$ (1–42) (Bachem) were pretreated by dissolving and incubating in HFIP (Wood et al., 1996). These solutions were stored at –80 °C. Just before use, aliquots of the HFIP solution were spin-dried, and the residue was dissolved in 0.1% HOAc.

For each series of experiments, a fresh aliquot of peptide was resuspended at 2 mg/mL in the 0.1% HOAc and diluted into the ApoE which had been dialyzed into PBS, 1 mM EDTA pH 7.4 at a 1:10 dilution or greater and incubated at room temperature for the times indicated. The incubated material was centrifuged in an Eppendorf microfuge (5 min, 14 000 RPM) to remove any large aggregates, passed through a 0.45  $\mu$ m Millipore Ultrafree-MC filter unit, and 50  $\mu$ L was loaded onto a Superose 12 PC3.2/30 column (Pharmacia) equilibrated with PBS/EDTA at 40  $\mu$ L/min. As assessed by dot blot quantitation and  $A_{280}$  (see below), recoveries of ApoE from chromatography (based on the amounts of ApoE and A $\beta$  in the complex mixtures *before* centrifugation and filtration) ranged from 70% to 90%, including experiments involving long incubation times and including experiments with the 1–42 version of A $\beta$ . As assessed by dot blotting, recoveries of A $\beta$ (1–40) ranged from 50% to 100%. Consistent with its greater tendency to aggregate, and hence be lost in the centrifugation step, recoveries of A $\beta$ (1–42) were in the range 10%–20%.

**Immunodetection and Quantitation of A $\beta$  and ApoE.** 50  $\mu$ L fractions from the gel filtration were collected and analyzed for A $\beta$  peptide and ApoE content by immunodetection. 5  $\mu$ L from each fraction was dotted onto nitrocellulose membranes (Schleicher & Schuell, Inc.). After air-drying, the membranes were moistened with distilled water and then blocked by swirling for 1 h in a solution of 5% non-fat dry milk in PBS containing 0.25% Triton X-100. Membranes were transferred into a dilution of either anti-A $\beta$  or anti-ApoE antibody into buffer A (0.5% non-fat dry milk in PBS containing 0.25% Triton X-100) and swirled

for 1 h. Membranes were washed in buffer A and then swirled for 1 h in a dilution of horseradish peroxidase-conjugated to an appropriate anti-immunoglobulin antibody (see below). Membranes were washed in buffer A and developed by ECL (Amersham). Reagents were as follows. For A $\beta$  detection: mouse monoclonal anti-A $\beta$  antibody 1E8 (SmithKline Beecham), recognizing amino acids 18–22 in the A $\beta$  peptide, at a dilution of 1:2000 from a 2 mg/mL solution, and goat anti-mouse IgG-HRP, at a dilution of 1:2000. For ApoE, polyclonal goat anti-human ApoE, at a dilution of 1–5000, and rabbit anti-goat IgG-HRP, at a dilution of 1:2000.

The A $\beta$  in the fractions was quantified from a standard dilution curve of the A $\beta$ (1–40) in the dot blots by densitometry with the Image 1000 and by visual inspection. ApoE levels were similarly estimated using the anti-ApoE antibody. In addition, ApoE was quantified by Bio-Rad protein assay using an ApoE standard (where its concentration was determined by amino acid composition) and also by using A<sub>280</sub> peak areas from the gel filtration. All three methods gave similar results.

## RESULTS

The human ApoE proteins were expressed under the IPTG inducible *tac* promoter and directed into the periplasmic space of *E. coli* by the *pelB* leader sequence. Expression of the full-length ApoE3 at 37 °C caused cell lysis. When the growth temperature was reduced to 32 °C, the cells remained intact and ApoE expression was about 5% of the total protein (Figure 1A). In contrast to the full-length protein, expression of the ApoE3 N-terminal domain at 37 °C did not appear to be toxic to *E. coli*, and expression was at least 20% of the total *E. coli* protein (Figure 1B). In both cases the ApoE accumulated solubly and could be released by osmotic shock, with the full-length protein located mostly in the water fraction and the ApoE N-terminus distributed between both the sucrose and the water fractions. The recovered yields after purification are about 2 mg/L for full-length ApoE3 and 8 mg/L for the ApoE3 N-terminal domain. N-terminal sequencing showed correct removal of the *pelB* signal, and mass spectrometry gave the expected molecular weight for both forms of ApoE3. Purification and characterization of the full-length E2 and E4 isoforms were similar to E3. Although ApoE3 contains one Cys residue and ApoE2 contains two, there appears to be no tendency for these proteins to make disulfide linked aggregates even when expressed at high levels in the periplasm, as shown by SDS-PAGE (Figure 1). The full-length ApoE isolated from *E. coli* co-migrates in SDS-PAGE with human plasma-derived ApoE (Calbiochem) (data not shown).

Figure 2 shows a series of chromatograms for various combinations of ApoE and A $\beta$ . ApoE3 run alone (Panel A, solid line) shows an A<sub>280</sub> trace consistent with its formation of a tetramer under native conditions. The elution position corresponds to a molecular weight of about 225 kDa (standard curve not shown), higher than the true molecular weight (about 136 kDa) but similar to values obtained previously by gel filtration analysis of the naturally derived protein and consistent with an elongated molecule (Yokoyama et al., 1985). Panel A (dashed line) also shows the A<sub>280</sub> trace for A $\beta$  alone, exhibiting only a small peak late in the chromatogram, as expected for A $\beta$ . When ApoE3 and A $\beta$

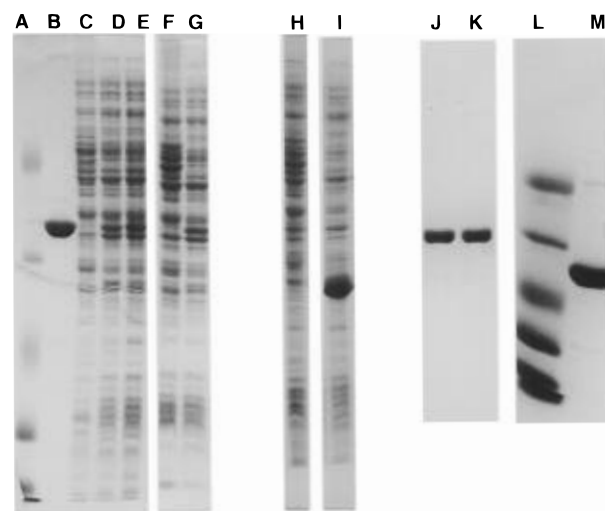


FIGURE 1: 12% SDS polyacrylamide gels (Laemmli, 1970) of ApoE samples and controls. Lanes A–I were run on 15 cm long slab gels; lanes J–M were run on a 7 cm minigel. Lanes A and L contain a low molecular weight protein standard mix, consisting of ovalbumin (43K), carbonic anhydrase (29K),  $\beta$ -lactoglobulin (18.4K), hen lysozyme (14.3K), pancreatic trypsin inhibitor (6.2K), insulin B chain (3K), and insulin A chain (2K). Lanes B–I summarize *E. coli* expression. Purified ApoE3 standard (B); *E. coli* containing control plasmid pTacII (no ApoE gene) after 3 h of growth post-induction (C, F, H); *E. coli* containing *tac* regulons with inserted ApoE cDNA after 3 h of growth post-induction, for ApoE2 (D), ApoE3 (E), ApoE4 (G), and the ApoE3 N-terminal domain (I). Lanes J, K, and M show the purity and absence of disulfide-linked dimers in *E. coli*-produced ApoE3. ApoE3 incubated with 40 mM iodoacetamide for 1 h at room temperature before adding gel loading buffer and running on gel (non-reduced sample, lane J); ApoE3 incubated in SDS gel loading buffer with 4 mM DTT for 1 h at 37 °C and then incubated with 40 mM iodoacetamide for 1 h at room temperature (reduced and alkylated sample, lane K); purified N-terminal domain of ApoE3 (lane M). Although it is generally not advisable to run reduced and non-reduced samples in adjacent gel lanes due to artifacts from diffusion of reducing agent between lanes, in the experiment depicted in lanes J and K there is no reducing agent present during electrophoresis, since the DTT sulfhydryls were alkylated by the excess iodoacetamide prior to gel loading.

are incubated together, however, then applied to the column, a new peak appears in the A<sub>280</sub> trace at an elution position near the void volume of the column (panel A, dotted line). As described below, this new peak contains immunoactivity indicative of the presence of both ApoE and A $\beta$ .

A number of methods were explored for quantitation of A $\beta$  in the column fractions. For example, the ApoE peak from chromatography of ApoE-A $\beta$  mixtures was subjected to SDS-PAGE followed by electrotransfer to nitrocellulose and immunochemical detection. Although it was clear from this analysis (data not shown) that significant amounts of A $\beta$  are present in the ApoE peak, quantitation proved impossible because of high backgrounds in the Western blot and variable recovery of the A $\beta$ , perhaps due to irreproducible, nonquantitative electrotransfer of this small, hydrophobic peptide. To avoid transfer losses, we investigated the use of simple dot blots in this defined system and were able to obtain reproducible results as described below. Although dot blot quantitation of complex mixtures can be compromised by nonspecific interactions of antibodies with other cellular components, in a simple defined system such as that described here the method proved to accurately represent the A $\beta$  content of column fractions.

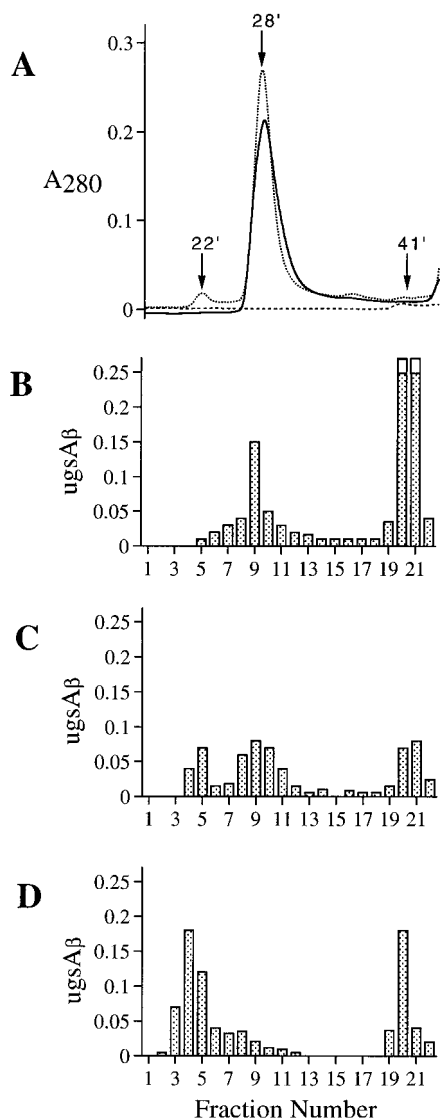


FIGURE 2: Superose 12 gel filtration profiles of ApoE3-A $\beta$ (1-40) co-incubations. Panel A,  $A_{280}$  profiles of A $\beta$  alone (---), ApoE3 alone (—) and an incubated mixture of A $\beta$  and ApoE3 (···). Panels B–D, analysis of A $\beta$  content of 5  $\mu$ L aliquots of each 50  $\mu$ L column fraction by the dot blotting procedure described in Materials and Methods and the legend to Figure 3. Panel B, 2 h incubation of 23  $\mu$ M HFIP-treated A $\beta$  and 5.4  $\mu$ M tetrameric ApoE3. Panel C, 4.5 h incubation of 46  $\mu$ M A $\beta$  and 5.8  $\mu$ M ApoE3. Panel D, 27 h incubation of 23  $\mu$ M A $\beta$  and 7  $\mu$ M ApoE3. Recoveries of A $\beta$  plotted are for 5  $\mu$ L aliquots of column fractions as described in Materials and Methods.

Figure 3 shows typical dot blot data for the quantitation of A $\beta$  in column fractions. Panel A shows the standard curve generated by blotting known amounts of A $\beta$ . Panel B shows the elution profile of A $\beta$  chromatographed alone. No trace of A $\beta$  is observed to elute earlier than the elution position of 41 min (fractions 19–21) consistent with a low molecular weight form<sup>2</sup> of the peptide. Panel C shows the dot blot analysis of column fractions from gel filtration of an ApoE–A $\beta$  comixture (the example corresponds to panel C in Figure 2). Digital integration analysis as well as visual inspection was used to assign quantities to each fraction based on standard curves run on the same blot. Different exposure times (not shown) were used to enhance the dynamic range of the assay.

Panels B–D of Figure 2 show three A $\beta$  elution profiles from gel filtration of different ApoE3 co-incubation experi-

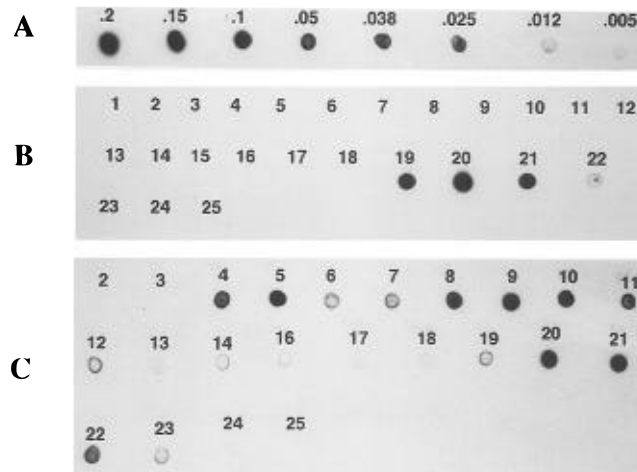


FIGURE 3: Dot blot analysis of standard curve and Superose 12 chromatography fractions using an anti-A $\beta$  antibody as described in Materials and Methods. Panel A, standard curve showing response of aliquots of A $\beta$ (1-40) in micrograms. Panel B, fractions of a chromatographic run of A $\beta$ (1-40) alone, corresponding to the profile shown in Figure 2, panel A. Column fractions were dotted underneath the number for that fraction; fractions 19–22 contain detectable amounts of A $\beta$ . Panel C, fractions of the chromatograph on the 4.5 h complex of ApoE3 and A $\beta$ , which gave rise to the profile shown in Figure 2C.

ments using the technique illustrated in Figure 3. Panel B shows the profile of a mixture chromatographed immediately after mixing and using A $\beta$ (1-40) which had previously been depleted of any residual aggregate by prior treatment with HFIP (Methods). The results show the A $\beta$  eluting in two locations, migrating with ApoE3 tetramer as well as at the position expected for the low molecular weight form<sup>2</sup> of A $\beta$  in aqueous solution. Quantitation of both A $\beta$  and ApoE in these fractions indicates a ratio of 3–4 mol of A $\beta$ (1-40) per mol of ApoE tetramer. Panel C shows the profile of a mixture using non-HFIP-treated A $\beta$ (1-40) and chromatographed after 2 h of incubation, in which A $\beta$  is found at the two positions occupied in panel B as well as at a third position corresponding to the high molecular weight peak seen in the  $A_{280}$  trace of the same reaction (Figure 2A). Panel D shows the profile of a similar mixture chromatographed after overnight incubation, showing that most of the A $\beta$ (1-40) by this time co-migrates with high molecular weight aggregate. The ratio of A $\beta$ (1-40) to ApoE in the high molecular weight complex populated at longer incubation times is much higher than that which co-elutes with the ApoE tetramer. For the 4 h incubation reaction shown in panel C, the ratio was calculated to be 94 mol of A $\beta$  per mol of ApoE tetramer, and for the 27 h incubation shown in panel D, 110 mol of A $\beta$  per mol of ApoE tetramer.

<sup>2</sup> The migration position we observe for A $\beta$  in the Superose chromatography is on the edge of the linear fractionation range for Superose 12, where the compactness of a peptide's conformation in native buffer would be expected to contribute substantially to its migration position and apparent molecular weight. Soreghan et al. (1994) have interpreted the migration of A $\beta$  in native gel filtration to indicate population of a dimeric structure. We do not feel our data can be used to address this question. While the aggregation state of A $\beta$  in aqueous solution at pH 7 is an important question, and will have implications, for example, for detailed models of how A $\beta$  interacts with ApoE at the molecular level, this aggregation state (i.e., monomer, dimer, or tetramer) is not critical to either the experimental design or interpretations of our paper, and we defer the question by referring to the form of A $\beta$  eluting around fraction 20 as the "low molecular weight form" of the peptide.

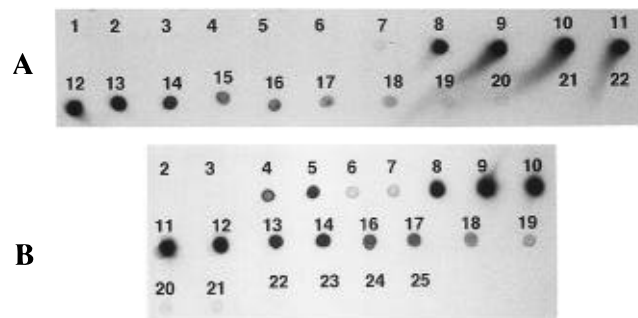


FIGURE 4: Dot blot analysis of Superose 12 chromatography fractions using an anti-ApoE antibody as described in Materials and Methods. Panel A, ApoE3 alone, corresponding to the run that generated the  $A_{280}$  trace shown in Figure 2A. Some trailing of the ApoE is apparent. Panel B, analysis of the fractions from chromatography of the complex obtained on incubating ApoE3 and A $\beta$  for 4.5 h. This is the same experiment as shown in Figure 2C.

Figure 4 shows that dot blotting could also be used to quantitate the ApoE levels in column fractions. Panel A shows the elution pattern for ApoE chromatographed alone and panel B the elution pattern for a co-incubation experiment (the one corresponding to panel C of Figure 2). ApoE levels were also estimated using  $A_{280}$  peak areas from the gel filtration run. Both assays relied on a standard ApoE solution independently quantified by amino acid composition analysis. The results from the dot blot analysis and integration of the ApoE  $A_{280}$  peak were in good agreement (data not shown).

A series of co-incubation/gel filtration experiments like those illustrated in Figure 2 were conducted with ApoE3 and A $\beta$ (1–40) at different incubation times. These experiments, as well as others described below, are summarized in Table 1. Figure 5 shows that progressively less A $\beta$  is isolated as part of the ApoE tetramer as incubation times increase, while more A $\beta$ (1–40) is isolated as part of the high molecular weight complex at longer incubation times.

The abilities of different isoforms of ApoE to promote the two classes of A $\beta$  complex were compared by conducting the gel filtration analysis of parallel incubation mixtures of each *E. coli*-produced isotype. Figure 6 shows the results for complex formation after 2 h of incubation. Table 1 summarizes all the experiments with different ApoE isoforms. The results indicate that all three isoforms are capable of supporting complex formation with both the ApoE tetramer and the higher molecular weight co-aggregate of ApoE and A $\beta$ . Although apparent differences exist, the differences do not appear to be significant and do not correlate with the observed genetic susceptibility of E4 > E3 > E2.

The N-terminal domain of ApoE3 was also produced in *E. coli* and purified from periplasmic extracts. Table 1 and Figure 7 summarize complex formation analysis with the purified domain. Panel A shows that the elution position of the  $A_{280}$  trace is later than that of the tetramer, corresponding to an estimated molecular weight of 68 Da (standard curve not shown). This is presumably higher than the expected molecular weight due to the elongated shape of this four-helix bundle (Wilson et al., 1991). Panels B and C show the A $\beta$  analysis of two co-incubation experiments incubated for either 3 h (B) or 21 h (C). The results show that the N-terminal domain of ApoE3 is capable of forming complexes of the monomeric N-terminal domain with A $\beta$  and

Table 1: Complex Formation Experiments

ApoE isoform <sup>a</sup>	[A $\beta$ ], $\mu\text{M}$ <sup>b</sup>	[ApoE], $\mu\text{M}$ <sup>c</sup>	time, h	A $\beta$ /ApoE <sup>d</sup>	
				22 min	28 min
3	46	6	2	66	9.1
3	46	5.8	4.5	94	6.7
3	23	6.5	2.5	116	0.8
3	11.4	7	2	107	0.4
3	23	7	2.5	107	1.1
3	23	7	8	110	0.5
3	46	6.5	24	67	1.0
3	23	7	27	110	0.6
3	23	7	0.16	ND	2.1
3	23	7	0.65	ND	1.3
2	46	6	4	88	3.9
2	11	6.5	2	ND	0.7
4	23	3.5	0.16	70	1.3
4	23	3.5	2.5	36	1.2
4	23	3.5	7.5	55	2.1
3 <sup>e</sup>	23	5.4	2	67	3.5
3	23	5.4	2	31	1.9
3 <sup>e</sup>	23	5.4	0.16	73	3.2
3	23	2.1	2	137	9.0
4	23	2.1	2	97	4.1
2	23	2.1	2	93	3.6
3	45	5.2	17	78	2.1
3	45	5.2	17	60	2.9
3NT <sup>f</sup>	46	24	3	ND	0.5
3NT <sup>f</sup>	46	24	21	ND	0.1
3 <sup>g</sup>	46	5.2	0.16	52	0.7
3 <sup>g</sup>	46	5.2	2	74	0.8

<sup>a</sup> Full-length isoform used except where designated. <sup>b</sup> All experiments with A $\beta$ (1–40) without HFIP treatment except where noted. <sup>c</sup> Concentration in terms of ApoE tetramer, except for those experiments using the N-terminal domain, which is monomeric. <sup>d</sup> In terms of ApoE tetramer, except for experiments with the monomeric N-terminal domain. <sup>e</sup> Experiments using HFIP-treated A $\beta$ (1–40). <sup>f</sup> Experiments using the N-terminal domain of ApoE3. <sup>g</sup> Experiments using A $\beta$ (1–42), pretreated with HFIP.

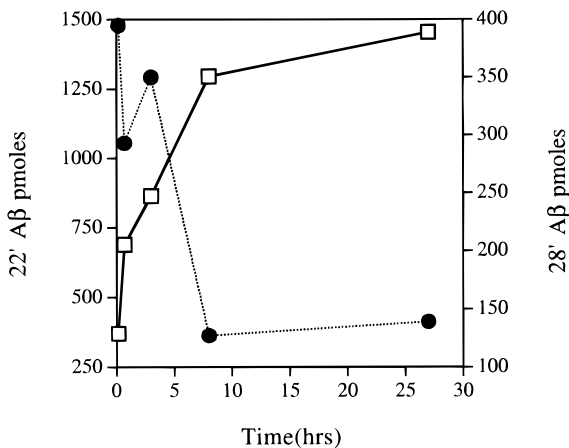


FIGURE 5: Time course of complex formation for both the ApoE tetramer-A $\beta$  complex (28 min peak, ●) and the high molecular weight ApoE-A $\beta$  complex (22 min peak, □). 23  $\mu\text{M}$  A $\beta$ (1–40) was incubated with 6  $\mu\text{M}$  ApoE3 in PBS, and at different time points an aliquot was taken for Superose 12 gel filtration and dot blot analysis.

higher molecular weight complexes. Much less complex is formed, however, than in comparable experiments with the full-length tetrameric protein, while most of the A $\beta$  continues to remain in solution and migrate in the monomer region, suggesting a weaker interaction of the N-terminal domain.

Although the binding of A $\beta$ (1–40) to the N-terminal domain of ApoE is less strong than that seen for full-length ApoE, it is probably significant. We ran two control proteins

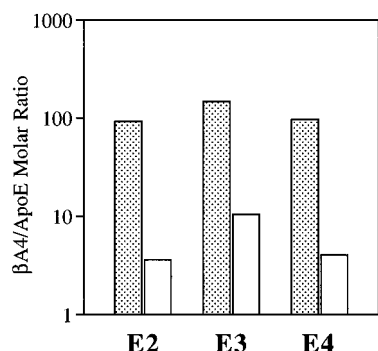


FIGURE 6: Complex formation between the ApoE isoforms and A $\beta$ (1–40). 23  $\mu$ M A $\beta$ (1–40) was incubated with 2.1  $\mu$ M ApoE for 2 h. After gel filtration, column fractions were quantified for both A $\beta$  and ApoE content and the ratio of A $\beta$  to ApoE was calculated for both the ApoE tetramer (open bars) and high molecular weight (stippled bars) complexes.

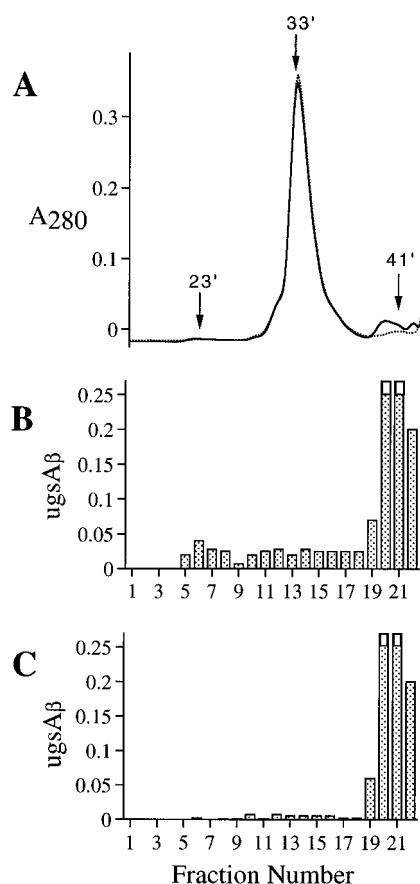


FIGURE 7: Complex formation between A $\beta$ (1–40) and the N-terminal domain of ApoE3. 46  $\mu$ M A $\beta$ (1–40) was mixed with 24  $\mu$ M ApoE3 N-terminus and incubated for 3 or 21 h at room temperature followed by dot blot analysis of A $\beta$  levels in column fractions. Panel A,  $A_{280}$  trace: ApoE alone ( $\cdots$ ), ApoE + A $\beta$  (—); panel B, A $\beta$  content of 3 h incubation; panel C, A $\beta$  content of 21 h incubation. Recoveries of A $\beta$  plotted are for 5  $\mu$ L aliquots of column fractions as described in Materials and Methods.

to ensure that co-migration of A $\beta$  with proteins is not a general property of this hydrophobic peptide. Proteins were incubated with A $\beta$ (1–40) and chromatographed as described for ApoE molecules. In these experiments, bovine serum albumin, a protein well-known for binding to hydrophobic molecules (Peters, 1985), was found to co-elute in native gel filtration chromatography with only 0.5% by weight of A $\beta$ . Analogously, a monoclonal IgG co-eluted with only 0.2% of A $\beta$  by weight. In contrast to these controls, the

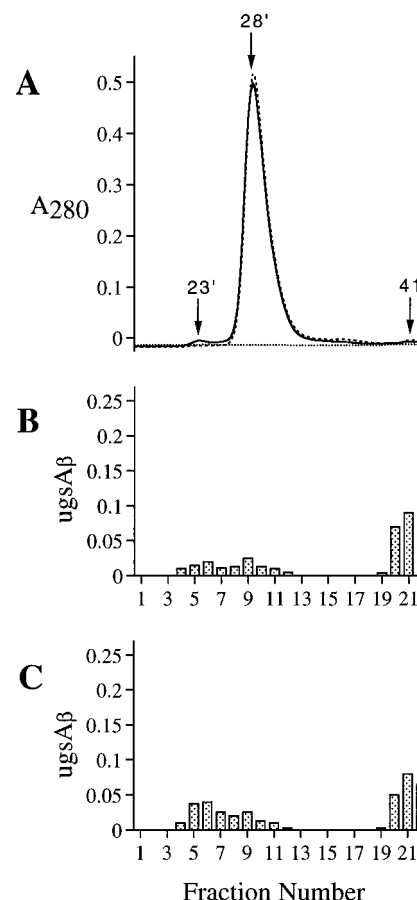


FIGURE 8: Superose 12 gel filtration profiles of ApoE3–A $\beta$ (1–42) co-incubations. Panel A, A $\beta$ (1–42) alone ( $\cdots$ ), ApoE3 alone ( $- -$ ), and a mixture of ApoE3 and A $\beta$ (1–42) after 10 min incubation (—). Panel B, A $\beta$  content of 5  $\mu$ L aliquots of 50  $\mu$ L column fractions of a mixture of 21  $\mu$ M ApoE3 and 46  $\mu$ M HFIP-treated A $\beta$ (1–42) after 10 min incubation. Panel C, the same mixture after 2 h incubation. Recoveries of A $\beta$  plotted are for 5  $\mu$ L aliquots of column fractions as described in Materials and Methods.

2–4 mol of A $\beta$ /mol of tetrameric ApoE seen in the early time points of many experiments with full-length ApoE isoforms corresponds to 6.5%–13% by weight. The weight percent of A $\beta$  carried by the N-terminal domain of ApoE3, 5.6%, is somewhat lower than the values seen for full-length ApoE but is considerably higher than the values for nonspecific binding of A $\beta$  to serum albumin or IgG.

Table 1 and Figure 8 summarize experiments exploring the ability of ApoE3 to form complexes with A $\beta$ (1–42), which is more hydrophobic and less-well-behaved than the 1–40 peptide. The A $\beta$  profiles for incubations of 10 min (Figure 8B) and 22 h (Figure 8C) show similar kinds of complex formation to that obtained in mixtures of ApoE and A $\beta$ (1–40). The poorer recoveries of A $\beta$  in these experiments, compared to comparable ones with the 1–40 peptide, can be attributed to greater losses of A $\beta$ (1–42) *via* precipitation during the incubation (Materials and Methods). This interpretation is consistent with the low recovery of unassociated A $\beta$ (1–42) seen in the chromatographic profiles.

## DISCUSSION

Several previously published studies suggest that ApoE is capable of binding A $\beta$ . Two groups reported staining of brain plaques with antibodies to ApoE (Namba et al., 1991;

Wisniewski & Frangione, 1992), but the inference that A $\beta$  in the plaque is responsible for binding, while reasonable, was not proven. More recently it was shown that biotinylated ApoE can bind to A $\beta$  fibrils generated *in vitro* (Sanan et al., 1994). Several studies have been interpreted to indicate an interaction between soluble forms of A $\beta$  and ApoE. Frangione and co-workers used an ELISA technique in which ApoE is nonspecifically immobilized on a plastic microtiter plate and A $\beta$  binding is detected using an anti-A $\beta$  antibody (Wisniewski et al., 1993). This method may be compromised, however, since proteins may become partially denatured after nonspecific non-covalent immobilization to surfaces (Van Regenmortel et al., 1988). Further, the assay is incapable of providing quantitative information on the molecular form of A $\beta$  which binds and the stoichiometry of binding. Strittmatter et al. (1993a,b) employed two different methods to demonstrate binding, both requiring that A $\beta$ -ApoE complexes survive exposure to the denaturant SDS. These methods suffer from the potential for the denaturing conditions used in the analyses to give data that does not reflect the native interaction. Even if the SDS-PAGE analysis of complex formation is accurately reporting on the existence of a non-covalent complex under native conditions, it is highly likely that the actual stoichiometry of binding, and the molecular forms of ApoE and A $\beta$  involved in that binding, might be obscured or altered by the denaturing conditions used in the analysis. Thus, to confirm and extend these previous reports, we have studied complex formation in the solution phase by generating and fractionating complexes under native buffer conditions.

Our data suggest the existence of two classes of ApoE-A $\beta$  complex. One complex (the 28 min aggregate) forms within the 10 min sample processing time of the gel filtration experiment and consists of the ApoE tetramer in complex with up to 4 mol of A $\beta$ . The best data for the composition of this complex come from experiments using A $\beta$  that was treated with the disaggregation agent HFIP (Wood et al., 1996) just prior to complex formation (Materials and Methods). This experiment (Figure 2B) was done twice using ApoE3, giving values for the number of molecules of A $\beta$  per ApoE tetramer of 3 and 4. In most other experiments, using all three ApoE isotypes under a variety of conditions, this ratio ranged down from a value of 4 (see, for example, Figure 5). In one experiment, involving incubation of high levels of A $\beta$  and ApoE3, a value of about 10 mol of A $\beta$  per ApoE tetramer was obtained; this high value might be exaggerated, however, due to an overlapping, higher molecular weight complex peak in the gel filtration.

Overall, the data suggests that each ApoE tetramer is capable of binding four molecules of A $\beta$  in this rapidly formed complex. That this stoichiometry is achieved by the formation of 1:1 complexes of A $\beta$  with each ApoE monomer is supported by the observation of weak and transient complex formation between A $\beta$  and the (monomeric) N-terminal domain of ApoE3 (Figure 7). However, it remains possible that the observed overall stoichiometry of binding by the ApoE tetramer might be obtained by other means: (1) each ApoE tetramer present might bind a single A $\beta$  tetramer or two A $\beta$  dimers (Soreghan et al., 1994) or (2) a fraction of the ApoE tetramers present might bind higher aggregates of A $\beta$ , with other ApoE tetramers binding nothing.

The second class of complex (the 22 min aggregate) forms more slowly on incubation at room temperature, constituting a significant portion of total ApoE-bound A $\beta$  after several hours. This complex, eluting at the void volume of the gel filtration column (>2000 kDa), continues to increase in amount until it constitutes, after 24 h, nearly all of the soluble A $\beta$  in the reaction mixture. Estimates of the stoichiometry of this complex are in the range 100–150 molecules of A $\beta$  per ApoE tetramer (Table 1). If this ratio reflected a complex involving a single ApoE tetramer, the aggregate molecular weight of such a complex would be about 600–800 kDa. The largest well-defined protein molecular weight standard we ran on our column, thyroglobulin, has a molecular weight of 670 000 and elutes at 23.5 min, clearly after the ApoE-A $\beta$  complex. The data therefore suggest that the high molecular weight aggregate of ApoE and A $\beta$  is a network involving more than one ApoE tetramer and hundreds of molecules of A $\beta$ . Long co-incubations of A $\beta$  and ApoE accumulate appreciable insoluble material, which is removed by centrifugation and filtration prior to gel filtration analysis. A Coomassie Blue-stained SDS gel of this precipitate shows it to contain both ApoE and A $\beta$  in comparable proportions to those found in the soluble aggregates (data not shown).

The most consistent interpretation of the data is that ApoE subunits possess a single binding site for A $\beta$  mediating rapid complex formation to yield a 4:1 stoichiometry of A $\beta$  to ApoE tetramer. Gradually a higher molecular weight complex forms containing stoichiometries of over 100:1, and eventually these latter complexes superaggregate and precipitate. The mechanism for the transition from the 28 min to the 22 min aggregate is not clear. The A $\beta$  molecules bound by the ApoE tetramer might serve as growth points for higher A $\beta$  aggregates. Alternatively, A $\beta$  aggregates that develop in solution without the mediation of ApoE (and which, in the absence of ApoE, would serve as seeds for rapid fibril growth) might be incorporated into ApoE complexes by exchange with, or addition to, the already bound A $\beta$  molecules.

We have shown that in fibril formation experiments driven by micromolar concentrations of A $\beta$ , relatively low (nanomolar) concentrations of ApoE can efficiently inhibit seeding of fibril formation (S. J. Wood, W. Chan, and R. Wetzel, unpublished). In contrast, at the relatively high concentrations of ApoE used in the experiments reported here, ApoE appears capable of recruiting solution phase A $\beta$  into soluble and insoluble co-aggregates. These co-aggregates bind thioflavin T and Congo red but are extremely inefficient at nucleating A $\beta$  fibril growth (S. J. Wood, W. Chan, and R. Wetzel, unpublished). Taken together, the data are consistent with a model in which ApoE and ApoE-A $\beta$  co-aggregates selectively recruit newly formed fibril nuclei from solution, thereby reducing their ability to initiate fibril growth.

Recently it was suggested that some results of experiments investigating ApoE-A $\beta$  interactions might be influenced by the choice of the molecular form of A $\beta$  used (Ma et al., 1994). To address this possibility, we repeated the complex formation experiments using ApoE3 and A $\beta$ (1–42). Figure 8 shows that results were obtained with A $\beta$ (1–42) which are similar to those from experiments using A $\beta$ (1–40). Using the same materials described here, this laboratory has also conducted experiments investigating the ApoE-A $\beta$  interaction by surface plasmon resonance (R. Wetzel and W. Chan unpublished) and by the ability of ApoE isotypes to inhibit

nucleation of A $\beta$  fibril formation (S. J. Wood, W. Chan, and R. Wetzel, unpublished). In both of these experimental systems, A $\beta$ (1–42) and A $\beta$ (1–40) generate similar results: (1) all three ApoE isotypes are capable of inhibiting seeding of fibril formation by exogenously applied A $\beta$  fibrils and (2) all three ApoE isotypes exhibit strong binding to fibril-like A $\beta$  aggregate immobilized on biosensor chips.

The molecular basis of the interaction of either monomeric or aggregated A $\beta$  with ApoE is not known. Models for the binding of ApoE and related apolipoproteins to lipoprotein particles suggest that the native helical bundles of ApoE might dissociate into their constituent amphipathic  $\alpha$ -helices, whose hydrophobic faces are thus free to associate with the hydrophobic edge of the lipoprotein particle disk (Weisgraber, 1994). It seems possible that a face of the growing A $\beta$  amyloid fibril might also display appreciable hydrophobicity and that binding of ApoE to this surface, perhaps in a manner similar to the proposed binding interaction with lipoprotein particles, would inhibit fibril extension.

The results presented here support the hypothesis that ApoE plays an important role in modulating the flux of A $\beta$  in the brain and hence the development of Alzheimer's disease. At the same time, our data do not present a plausible explanation for the correlation of ApoE genotype with Alzheimer's disease risk. It may be that the ApoE–A $\beta$  complex formation and fibril formation inhibition we observe accurately reflects the role of ApoE in the disease process but that the disease genetics arise due to additional factors (Evans et al., 1995). For example, allelic differences in expression levels of ApoE observed in the circulation (Gregg et al., 1986) might also occur in the brain, or the different isoforms may interact differently when, loaded with A $\beta$ , they interact with cell surface receptors. The different abilities of the three isoforms to form disulfide bonds might also contribute to the observed genetics (Evans et al., 1995). Lipid loading might also introduce or enhance differences in the abilities of ApoE isoforms to influence A $\beta$  flux and aggregation (LaDu et al., 1995).

## ACKNOWLEDGMENT

We gratefully acknowledge Steve Holmes for a sample of the anti-A $\beta$  antibody 1E8 and Nabil Elshourbagy for the ApoE3 cDNA clone.

## REFERENCES

- Castano, E. M., Prelli, F., Wisniewski, T., Golabek, A., Kumar, R. A., Soto, C., & Frangione, B. (1995) *Biochem. J.* 306, 599–604.
- Corder, E. H., Saunders, A. M., Strittmatter, W. J., Schmechel, D. E., Gaskell, P. C., Small, G. W., Roses, A. D., Haines, J. L., & Pericak-Vance, M. A. (1993) *Science* 261, 921–923.
- Evans, K. C., Berger, E. P., Cho, C.-G., Weisgraber, K. H., & Lansbury, P. T., Jr. (1995) *Proc. Natl. Acad. Sci. U.S.A.* 92, 763–767.
- Gregg, R. E., Zech, L. A., Schaefer, E. J., Stark, D., Wilson, D., & Brewer, H. B., Jr. (1986) *J. Clin. Invest.* 78, 815–821.
- Hilbich, C., Kisters, W. B., Reed, J., Masters, C. L., & Beyreuther, K. (1991) *J. Mol. Biol.* 218, 149–163.
- Kirschner, D. A., Inouye, H., Duffy, L. K., Sinclair, A., Lind, M., & Selkoe, D. J. (1987) *Proc. Natl. Acad. Sci. U.S.A.* 84, 6953–6957.
- LaDu, M. J., Falduto, M. T., Manelli, A. M., Reardon, C. A., Getz, G. S., & Frail, D. E. (1994) *J. Biol. Chem.* 269, 23403–23406.
- LaDu, M. J., Pederson, T. M., Frail, D. E., Reardon, C. A., Getz, G. S., & Falduto, M. T. (1995) *J. Biol. Chem.* 270, 9039–9042.
- Laemmli, U. K. (1970) *Nature* 227, 680–685.
- Ma, J., Yee, A., Brewer, H. J., Das, S., & Potter, H. (1994) *Nature* 372, 92–94.
- Namba, Y., Tomonaga, M., Kawasaki, H., Otomo, E., & Ikeda, K. (1991) *Brain Res.* 541, 163–166.
- Peters, T. (1985) In *Advances in Protein Chemistry* (Anfinsen, C. B., Edsall, J. T., & Richards, F. M., Eds.) pp 161–245, Academic Press, San Diego, CA.
- Sambrook, J., Fritsch, E. F., & Maniatis, T. (1989) *Molecular Cloning: A Laboratory Manual*, Cold Spring Harbor Laboratory Press, Cold Spring Harbor, NY.
- Sanan, D. A., Weisgraber, K. H., Russell, S. J., Mahley, R. W., Huang, D., Saunders, A., Schmechel, D., Wisniewski, T., Frangione, B., Roses, A. D., & Strittmatter, W. J. (1994) *J. Clin. Invest.* 94, 860–869.
- Selkoe, D. J. (1995) *Nature* 375, 734–735.
- Soreghan, B., Kosmoski, J., & Glabe, C. (1994) *J. Biol. Chem.* 269, 1–5.
- Strittmatter, W. J., Saunders, A. M., Schmechel, D., Pericak-Vance, M., Enghild, J., Salvesen, G. S., & Roses, A. D. (1993a) *Proc. Natl. Acad. Sci. U.S.A.* 90, 1977–1981.
- Strittmatter, W. J., Weisgraber, K. H., Huang, D. Y., Dong, L.-M., Salvesen, G. S., Pericak-Vance, M., Schmechel, D., Saunders, A. M., Goldgraber, D., & Roses, A. D. (1993b) *Proc. Natl. Acad. Sci. U.S.A.* 90, 8098–8102.
- Van Regenmortel, M. H. V., Briand, J. P., Muller, S., & Plaue, S. (1988) *Synthetic Polypeptides as Antigens*, Elsevier, Amsterdam.
- Weisgraber, K. H. (1994) In *Advances in Protein Chemistry* (Schumaker, V. N., Ed.) pp 249–302, Academic Press, San Diego, CA.
- Wilson, C., Wardell, M. R., Weisgraber, K. H., Mahley, R. W., & Agard, D. A. (1991) *Science* 252, 1817–1822.
- Wisniewski, T., & Frangione, B. (1992) *Neurosci. Lett.* 135, 235–238.
- Wisniewski, T., Castano, E. M., Golabek, A., Vogel, T., & Frangione, B. (1994) *Am. J. Pathol.* 145, 1030–1035.
- Wisniewski, T., Golabek, A., Matsubara, E., Ghiso, J., & Frangione, B. (1993) *Biochem. Biophys. Res. Commun.* 192, 359–365.
- Wood, S. J., Maleeff, B., Hart, T., & Wetzel, R. (1996) *J. Mol. Biol.* 256, 870–877.
- Yokoyama, S., Kawai, Y., Tajima, S., & Yamamoto, A. (1985) *J. Biol. Chem.* 260, 16375–16382.

BI952852V